Optical re-injection in cavity-enhanced absorption spectroscopy

J. Brian Leen[a] and Anthony O'Keefe
Los Gatos Research, 67 E. Evelyn Avenue, Suite 3, Mountain View, California 94041, USA

(Received 11 February 2014; accepted 12 August 2014; published online 2 September 2014)

Non-mode-matched cavity-enhanced absorption spectrometry (e.g., cavity ringdown spectroscopy and integrated cavity output spectroscopy) is commonly used for the ultrasensitive detection of trace gases. These techniques are attractive for their simplicity and robustness, but their performance may be limited by the reflection of light from the front mirror and the resulting low optical transmission. Although this low transmitted power can sometimes be overcome with higher power lasers and lower noise detectors (e.g., in the near-infrared), many regimes exist where the available light intensity or photodetector sensitivity limits instrument performance (e.g., in the mid-infrared). In this article, we describe a method of repeatedly re-injecting light reflected off the front mirror of the optical cavity to boost the cavity's circulating power and deliver more light to the photodetector and thus increase the signal-to-noise ratio of the absorption measurement. We model and experimentally demonstrate the method's performance using off-axis cavity ringdown spectroscopy (OA-CRDS) with a broadly tunable external cavity quantum cascade laser. The power coupled through the cavity to the detector is increased by a factor of 22.5. The cavity loss is measured with a precision of 2×10^{-10} cm$^{-1}/\sqrt{\text{Hz}}$; an increase of 12 times over the standard off-axis configuration without reinjection and comparable to the best reported sensitivities in the mid-infrared. Finally, the re-injected CRDS system is used to measure the spectrum of several volatile organic compounds, demonstrating the improved ability to resolve weakly absorbing spectroscopic features. © *2014 AIP Publishing LLC*. [http://dx.doi.org/10.1063/1.4893972]

INTRODUCTION

The detection of trace gas constituents at concentrations of parts-per-billion (ppb) or lower is required for many applications, including environmental and atmospheric science,[1] industrial process control,[2] and medical breath diagnostics.[3,4] Conventional absorption spectroscopy (CAS) is a powerful analytical technique that allows the quantitative speciation of gas mixtures, but typically lacks the sensitivity required to detect ppb or ppt concentrations. Cavity ringdown spectroscopy (CRDS),[5] integrated cavity output spectroscopy (ICOS),[6–8] and other cavity-enhanced absorption spectrometry techniques[9,10] are commonly used to detect and quantify analytes at concentrations that are undetectable by CAS. These techniques improve on CAS by using a high-finesse optical cavity to increase the interaction length between the probe light and the gas sample.[11,12]

CRDS and ICOS in the mid-infrared (MIR) spectral region are particularly attractive because, in addition to long path lengths, they exploit strong optical absorptions associated with fundamental rotational-vibrational transitions. These transitions have absorption cross sections orders of magnitude larger than in the near-infrared and provide molecular "fingerprints" of target analytes.[13] There are numerous implementations of CRDS and ICOS that take advantage of the strong, unique absorptions in the MIR. Whittaker *et al.* coupled difference frequency generation (DFG) sources with CRDS in the 3 μm region to achieve a minimum detectable absorption (MDA) of 2.9×10^{-9} cm^{-1} in 44 s.[14] Peltola *et al.* used a continuous wave optical parametric oscillator (cw-OPO) operating near 3.4 μm in conjunction with re-entrant CRDS to achieve an MDA of 1.5×10^{-8} cm^{-1} in 2 s.[15] Recent improvements in quantum cascade lasers (QCLs) offering higher power (tens to hundreds of milliwatts), room temperature lasing and good beam quality have led to a rapid increase in the number of instruments for the sensitive and specific measurement of trace gases in the MIR.[13,16–18] Ciaffoni *et al.* utilized a QCL with cavity enhanced Fourier-transform spectroscopy for the detection of acetone with a limit of detection (LOD) of 510 ppb.[19] Gorrotxategi-Carbajo *et al.* used optical feedback cavity enhanced spectroscopy to achieve an MDA of 5×10^{-10} cm^{-1} in 1 s.[20]

Of special interest is the external cavity quantum cascade laser (EC-QCL), which can tune over many microns (5-14 μm) allowing unprecedented spectral coverage.[21] Unfortunately, EC-QCLs capable of tuning over the widest spectral range also have a wide spectral bandwidth (~0.5 cm^{-1}), which makes them unsuitable for high resolution optical spectroscopy (e.g., single rotational-vibrational transitions of molecules with 2-5 atoms). However, EC-QCL's broad spectral range offers the opportunity to measure the broad absorption spectra of larger volatile organic compounds (VOCs) for which individual rotational-vibrational transitions are merged into a continuous absorption band. An EC-QCL used in conjunction with CRDS has previously been demonstrated for the detection of chemical warfare agent (CWA) simulants (i.e., dimethyl methylphosphonate (DMMP)), achieving an absorption sensitivity of 2×10^{-7} cm^{-1}.[22] This yielded a detection limit 6.7 ppb of sarin, which was significantly higher than the roughly 1 ppb minimum detectable concentration

[a]Author to whom correspondence should be addressed. Electronic mail: b.leen@lgrinc.com

required for CWA alarms.[23] VOCs such as BTEX (benzene, toluene, ethylbenzene, and isomers of xylene), trichloroethylene, and tetrachloroethylene and CWA (e.g., sarin, vx, soman, and tabun)[24,25] are important examples of VOCs that can be detected at low or sub- part-per-billion (ppb) levels with the instrument described in this article.

The best CRDS sensitivity is typically achieved when the source laser is mode-matched to the cavity's lowest order transverse mode and frequency-locked to the cavity's longitudinal modes, resulting in stable ringdowns and high optical transmission to the detector. Unfortunately, mode-matching is extremely sensitive to environmental factors such as temperature and pressure variations and mechanical vibrations. As a result, the off-axis (OA) configuration was developed to forego high optical transmission in favor of a more robust system.[26] OA alignments, which can be applied to either CRDS or ICOS, reduce mode noise by coupling to many higher-order transverse modes, in effect, decreasing the cavity's free spectral range. This method has been used extensively in the MIR with ICOS to measure trace gases.[17,18,27,28] The primary advantage of OA-ICOS is the ease of implementation and robust field performance, making the instruments relatively inexpensive, and ideal for remote and airborne applications.

The downside of the OA configuration is that the transmission through the cavity and onto the detector decreases to a value on the order of the mirror transmission (typically on the order of 0.01% of the incident light beam). The decreasing optical signal with increasing mirror reflectivity forces a tradeoff between path length and noise that ultimately limits system performance.[29] This is particularly true in the MIR where HgCdTe (MCT) detectors must be cooled to cryogenic temperatures to achieve optimum performance. Additionally, mirror performance is relatively poor (absorption $\gtrsim$500 ppm) above 8 μm and very poor (absorption $\gtrsim$1000 ppm) above 12 μm due to material absorptions in the dielectric stack.[30]

In this article, we present a method of increasing the power injected into an OA cavity by using an inexpensive metal mirror to repeatedly re-inject the light reflected from the front cavity mirror.[31] The method is applicable as a simple addition to many cavity-enhanced absorption techniques and we demonstrate its utility in conjunction with a broadly tunable EC-QCL for the detection of trace VOCs. Because EC-QCLs are typically pulsed and have power fluctuations of 1% they are best suited to CRDS and we use an OA-CRDS setup for demonstration of the re-injection principle. Using this configuration we are able to achieve an MDA lower than many previously reported values for cavity enhanced absorption spectroscopy in the MIR and 2 orders of magnitude better than previously published EC-QCL CRDS sensitivity.[22]

OPTICAL CONFIGURATION

Figure 1 shows a diagram of a re-injected OA-CRDS setup. The sample cell has 2″ diameter, high reflectivity mirrors with a 1 m radius of curvature (II-VI Infrared) and a separation of 80.3 cm. Each mirror has a per-reflection loss (due to transmission, absorption and scattering) of 800–2000 parts per million over the spectral range from 960–1290 cm^{-1}.

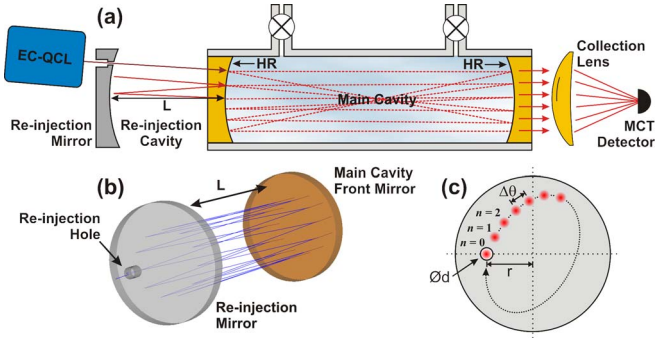

FIG. 1. (a) Schematic of the re-injected OA-CRDS cavity. The EC-QCL beam is introduced through a hole in the re-injection mirror. The re-injection cavity is separated from the main cavity by a distance L. The gas sample under test is contained exclusively in the main cavity. (b) 3D ray pattern in the reinjection cavity. (c) Diagram of the spot pattern on the re-injection mirror. The injection hole has a diameter d and is offset from mirror center by a distance r. The beam precesses in an ellipse around the perimeter of the mirror, separated from the previous spot by an advance angle $\Delta\theta$.

Gas flow into and out of the cell is controlled using two all-Teflon solenoid valves (Neptune Research) that enable sample and hold measurement of selected gas volumes. Light from the exit mirror is collected using a 2″ diameter, f/0.85, ZnSe meniscus lens. The detector is a liquid nitrogen cooled, photovoltaic HgCdTe with a 1 mm element size (J19D11, Teledyne-Judson) amplified by a custom, bootstrapped transimpedance amplifier with a bandwidth of 2 MHz and a gain of 5×10^4 V/A (FEMTO Messtechnik GmbH).[32]

The laser source is a pulsed EC-QCL (LaserTune, Block Engineering) that is capable of tuning from 830 to 1430 cm^{-1} (7–12 μm). The laser's pulse width is 500 ns at a rate of 62.5 kHz and has an average power of between 0.5 and 12 mW. Each pulse has a spectral width of approximately 0.5 cm^{-1}, which is significantly larger than the cavity free spectral range of 0.006 cm^{-1} and results in transmission through coupling into multiple longitudinal cavity modes. Each laser pulse produces a ringdown event with a time constant, τ, dictated by the standard CRDS equation:[33]

$$\tau(\nu) = \frac{l}{c[(1-R)+\alpha(\nu)l]}, \quad (1)$$

where l is the cavity length, c is the speed of light, $\alpha(\nu)$ is the absorption due to the gas sample at wavenumber ν, and R is the cavity mirror reflectivity. The ringdown is digitized at 10 MSamples/s (National Instruments PCI-6115) and fit using optimal Levenberg-Marquardt least squares minimization.[34] The cavity is filled with ultra-zero air and the baseline ringdown, τ_0, is measured across the usable mirror band. Finally, the loss attributable to any introduced gas is calculated according to

$$\alpha(\nu) = \frac{1}{c}\left(\frac{1}{\tau(\nu)} - \frac{1}{\tau_0(\nu)}\right). \quad (2)$$

Re-injection of the light reflected from the main cavity mirror is achieved using a silver coated mirror (the re-injection mirror or RIM) with a reflectivity of 98% and a 50 cm radius of curvature. To permit the initial injection of light, a 4.8 mm hole is drilled 12 mm from the mirror center. The hole size is chosen to minimize clipping of the EC-QCL

beam, which has a $1/e^2$ size of 2.1 × 1.8 mm. Initially, the beam passes through the injection hole and is incident on the main cavity mirror where a small portion of the beam (∼0.1%) is transmitted through to the main cell. The rejected light (∼99.9%) is repeatedly retro-reflected by the RIM back into the main cavity, adding to the circulating power. The re-injection cavity formed by the re-injection mirror and the main cavity front mirror is similar to a Herriott cell[35] (Figure 1(b)) and the re-injection performance is dictated by the number of reflections that occur before the beam becomes re-entrant and passes back out of the injection hole. The length of the re-injection cavity should be kept within the stability region $0 \leq \left(1 - {}^{L}/_{R_{RIM}}\right)\left(1 - {}^{L}/_{R_{F}}\right) \leq 1$, where L is the re-injection cavity length, R_{RIM} is the radius of the RIM, and R_F is the radius of the main cavity front mirror.[36] For the radii studied here, the stability region extends from L = 0 to 500 mm. The beam pattern is typically elliptical where each reflection is offset by an advance angle $\Delta\theta$ as shown in Figure 1(c). Although not explored here, an astigmatic RIM offers the potential to greatly increase the injected power in a manner analogous to astigmatic Herriott cells.[37,38]

An example of the increase in incident power on the detector with re-injection is shown in Figure 2(b), which depicts the measured ringdowns and exponential fit with and without optimized re-injection at ν = 1100 cm^{-1}. The noise (as shown by the fit residual in panel (a)) is far from the shot noise limit and is equivalent for both cases. The amplitude of the re-injected case is 20 times larger than the single beam injection resulting in the signal-to-noise ratio (SNR) increasing from 17:1 to 329:1. Under conditions of low SNR that frequently occur in the MIR spectral region, this improvement in signal amplitude results in significantly lower noise on the fit estimate of the ringdown time and thus on the estimate of optical absorption, $\alpha(\nu)$.

SIMULATION OF RE-INJECTION PERFORMANCE

In practice, calculating the re-injection efficiency is much more complicated than estimating the loss from each reflection within the re-injection cavity. Because the figure of merit is power incident on the detector element, propagation through all the optical elements must be considered to obtain a reasonable estimate of re-injection efficiency. We have defined the re-injection efficiency as the ringdown fit amplitude with the re-injection mirror normalized by the fit amplitude when the re-injection mirror is removed. The experimental optical train was modeled using non-sequential ray tracing in Zemax (Radiant Zemax), wherein rays are split according to reflected and transmitted power at each optical interface. By eliminating rays that fall outside the aperture of any optic, this method properly accounts for rays that constitute bad injections (e.g., rays that strike the main cavity walls) or that do not strike the detector. Although this calculation is incomplete in that it does not include diffraction effects (which are important when beams fall near to the main cavity walls[39]), it provides a quantitatively and qualitatively accurate prediction of the re-injection efficiency.

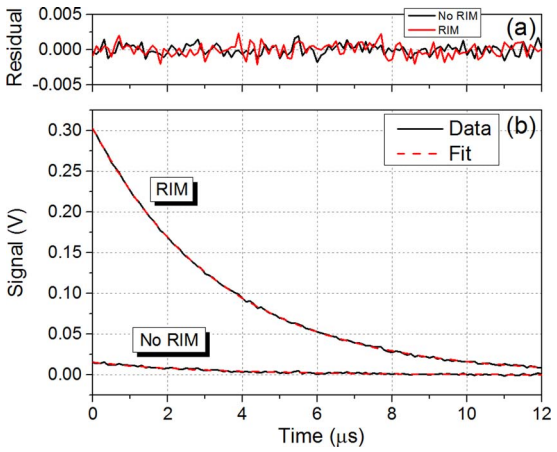

FIG. 2. Experimentally measured ringdown events both with and without the re-injection mirror. The signal amplitude is 20 times larger with the RIM, but the noise is equivalent. (a) shows the fit residuals, and (b) shows the measured data fit to a single decaying exponential.

The simulation is identically configured to the experimental setup, having the same mirror curvatures, clear apertures, re-injection hole size and offset, beam diameter and divergence, collection lens surfaces, and detector size. The exception is the main cavity reflectivity, which must be reduced to limit the computational complexity from multiple low loss reflections. As in the experimental case, the angular alignment of the injected beam is varied at a fixed re-injection cavity length, L (see Figure 1) and an optimum alignment is achieved when the power transmitted to the detector is a maximum.

It is worth considering the expected re-injection efficiency between 0 and 500 mm. At small L, the injected beam incident angle must be large so that the first reflection misses the injection hole. Unfortunately, large incident angles into the re-injection cavity also result in large angles into the main cavity, which strike the wall because of the long main cavity length (803 mm) and result in zero injected power. At moderate L, the efficiency will reach a maximum where the injection angle is small enough to be accepted by the main cavity and $\Delta\theta \cdot$ L is approximately equal to the beam width. As L increases, the radius of the precession pattern on the main cavity mirror increases and the pattern will be clipped by the main cavity aperture.

We have simulated and experimentally measured the reinjection behavior *versus* L for two injection beam angular alignments; one where the angle is optimized at L = 100 mm, and another at L = 200 mm. The results are shown in Figure 3 where L is varied between 40 and 280 mm. Figure 3 shows the expected behavior with good agreement between the experimental and simulated results. The total re-injection efficiency is lower for the experimental case than the simulation, likely because of the diffraction effects at the main cavity walls which are particularly severe for the larger pattern produced by the optimization at L = 200 mm. The re-injection efficiency optimized at L = 100 mm is significantly higher and is used throughout the remainder of this article.

The re-injection efficiency shows an oscillating structure at longer L that is due to periodic phase matching of the spot pattern with the re-injection hole (i.e., minima occur at $2\pi = N\Delta\theta$). Fringes in the 100 mm optimized case have slightly

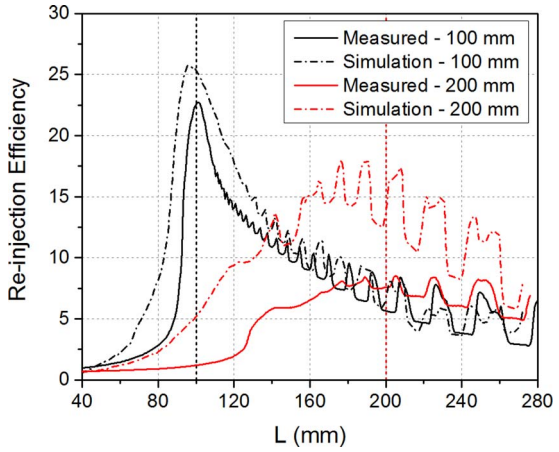

FIG. 3. Comparison of simulated and measured re-injection efficiency vs. re-injection cavity length, L. Black (red) traces show data for injection angle optimized at L = 100 mm (200 mm). The two optimization locations are marked with dashed vertical lines of corresponding color. The phase shift between the curves optimized at 100 mm is due to a slight difference in r.

different periods because the re-injection mirror center is not rigidly enforced in the experimental setup, which can lead to a small effective change in r and thus $\Delta\theta$. The good agreement between simulation and experiment indicate that the ray tracing model will be a useful tool for future optimization of the re-injection configuration.

EXPERIMENTAL IMPROVEMENT IN SNR

Single wavelength precision

The key benefit of the re-injection configuration is its ability to improve the precision of the cavity ringdown measurement. Figure 4 shows the experimental improvement in the optical loss determination ($1/c\tau$), measured at a single laser frequency (1100 cm^{-1}) for 7 h. The cell is filled with 600 Torr of ultra-zero air (Airgas). Figure 4(a) shows a significant improvement in the peak-to-peak noise with the re-injection mirror. The Allan deviation in Figure 4(b) shows the measurement precision for various data averaging time periods. The improvement in precision is greatest at short time scales and decreases as thermal and mechanical fluctuations cause alignment changes that result in variations of the actual system optical loss. For example, the degradation in precision for the re-injection case occurring at 700 s is a result of temperature fluctuations due to air conditioning cycles with a period of 10-30 min. This oscillation can be seen clearly in the loss trace, particularly during the first 2 h where the cycles occur more frequently. Note that, due to the large noise on the non-re-injected data, the air conditioning cycles cannot be discerned. At the very longest time scales, the precision of the two cases converge, indicating that changes to optical alignment, rather than noise on the ringdown fit dominate the precision beyond about 5000 s.

Spectrum measurement precision

Because the tuning mechanism for EC-QCLs is mechanical (i.e., a moving grating), spectra are collected using a "step and measure" procedure where the laser is commanded to a wavenumber and, after a small tuning delay, the ringdown is measured. For quantitative measurements of trace gas concentrations, the relevant metric is the precision *versus* wavenumber during the acquisition of absorption spectra. Figure 5(a) shows the optical loss measurement precision (1σ) at each wavenumber across the cavity's accessible mirror band. For these measurements, the cavity was filled with ultra-zero air at 600 Torr and the measurement time per spectrum is 9 min, with a 0.5 cm^{-1} step size, a tuning delay of 250 ms, and a collection of 20 000 ringdowns for each step. The measurement precision degrades at the mirror band edges because the cavity ringdown times become short (<1 μs), limiting the number of data points per τ and resulting in an increase in fit uncertainty. Figure 5(b) compares the measured ringdown

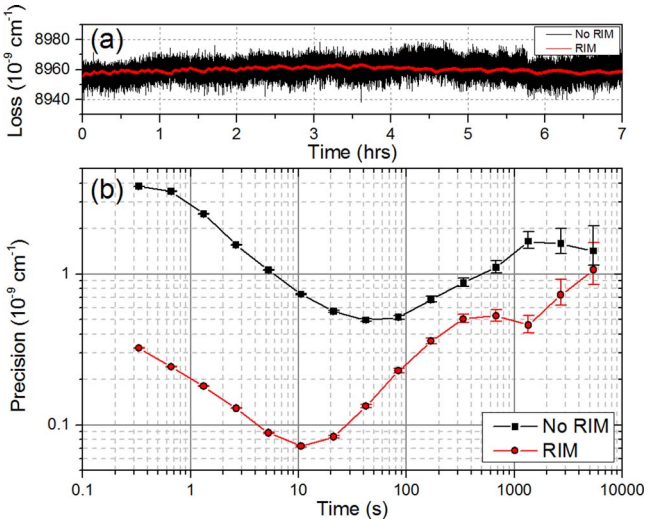

FIG. 4. (a) Measured loss with and without re-injection at 1100 cm^{-1} with 600 Torr of ultra-zero air. (b) Allan deviation of the loss time trace above showing the precision at various averaging time scales.

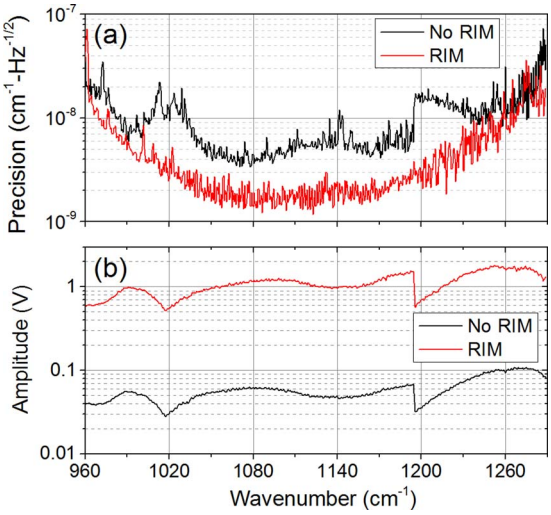

FIG. 5. (a) The measured precision vs. wavenumber with and without the re-injection mirror. The cavity is filled with 600 Torr of ultra-zero air. (b) The measured ringdown amplitude corresponding to (a). Discontinuities occur when the laser switches gain media.

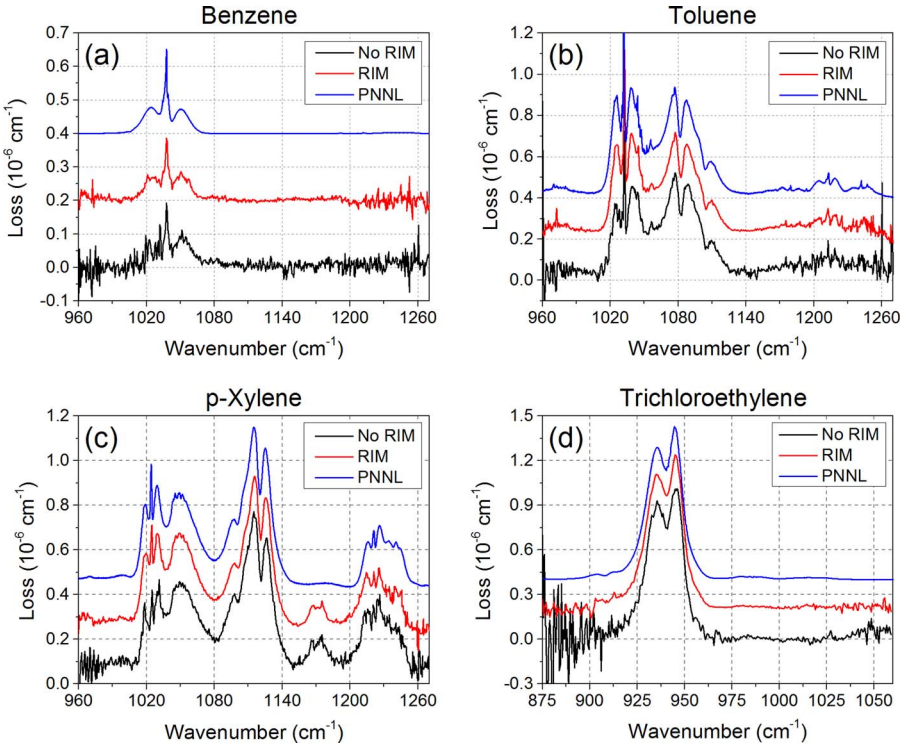

FIG. 6. Absorption spectra of selected VOCs at 600 Torr measured with and without the re-injection mirror. (a) 104 ppb benzene, (b) 992 ppb toluene, (c) 955 ppb p-xylene, and (d) 88.7 ppb trichloroethylene. PNNL library spectra are shown in blue for reference. Each spectrum is vertically offset by 2.0×10^{-6} cm^{-1} to improve visibility. (d) is measured with an alternative mirror pair the covers 875–1060 cm^{-1}. Note that the p-xylene mixture is contaminated with an unknown compound absorbing at 1170 cm^{-1}.

amplitude across the spectrum. Note that discontinuities are present where the laser switches from one QCL gain chip to another. For the non-re-injected case, the precision is inversely correlated to the ringdown fit amplitude, clearly indicating that the instrument's performance is limited by the laser power. Conversely, the re-injected case shows an increase in ringdown fit amplitude of 20×, resulting in an improvement in precision from 1×10^{-8} cm^{-1} to 3×10^{-9} cm^{-1} in the center of the mirror band. This relatively small proportional improvement in precision is consistent with the results shown in Figure 4(b) around 9 min (540 s). However, the precision on the measured spectrum in Figure 5(a) is worse (both with and without the re-injection) than the precision measured at a single wavelength in Figure 4, likely because of additional systematic noise resulting from tuning the laser (e.g., slightly different actual wavenumber or variable spectral envelope).

Spectra of trace VOCs

In order to demonstrate the improved ability to resolve weak optical absorptions using re-injection, we have measured the cavity-enhanced spectra of several important volatile organic compounds (VOCs) with and without re-injection. The VOCs were prepared at trace concentrations (100 ppb–1 ppm; NIST-traceable) in ultra-zero air (Scott-Marrin) with uncertainties of 2% (toluene and p-xylene), 5% (benzene), and 10% (trichloroethylene). All measurements were made on a static sample volume at 600 Torr using the same measurement parameters as Figure 5. The results are shown in Figure 6. Note that many spectral features that are absent or noisy when measured without re-injection are clearly resolved when measured with re-injection. Spectra recorded with high-resolution FTIR from the Pacific Northwest National Laboratory (PNNL) library[40] are included for comparison and confirm that the results obtained with re-injection accurately resolve the absorption spectra. Figure 6(d) is taken with a different mirror set that covers the spectral range from 875–1060 cm^{-1}. Specific examples of improved resolving power include: in Figure 6(a) the P-branch of the benzene absorption, in Figure 6(b) the toluene P-branch at 1030 cm^{-1} and the P, Q, R set at 1215 cm^{-1}, in Figure 6(c) the p-xylene P-branch at 1020 cm^{-1} and the P, Q, R set at 1220 cm^{-1}, and in Figure 6(d) the noise on trichloroethylene peak and the baseline noise. In each of the plots in Figure 6, the improved spectrum SNR with re-injection will aid in the quantitative estimation of analyte concentration.

CONCLUSION

We have described a method of increasing power transmission and signal-to-noise ratio in OA-CRDS by a factor of 22.5 by repeatedly re-injecting the light reflected from the front cavity mirror. Ray tracing simulations of the re-injected cavity are in good agreement with experimental results and, in the future, can be used to further optimize the re-injection efficiency by adjusting mirror parameters, including the introduction of astigmatism that will result in >100 re-injections.[38] The experimental OA-CRDS system achieved a loss measurement precision of 2×10^{-10} cm$^{-1}/\sqrt{\text{Hz}}$; with re-injection, which was shown to improve the instrument's

resolving power of weak absorbers. When used to measure ultra-trace concentrations or complicated mixtures, the increased resolving power will lead to improved sensitivity and specificity. Additionally, the increase in transmitted power permits the use of non-cryogenic detectors (e.g., thermoelectrically cooled), greatly increasing the ease of use and portability of trace gas analyzers for applications such as indoor air quality monitoring, breath analysis, and chemical weapons detection. In other wavelength regions, the re-injection method will allow the use of lower power, less costly lasers or higher reflectivity mirrors that provide much longer optical path lengths while maintaining the same signal amplitude. Finally, the simpler, more robust nature of OA-CRDS or OA-ICOS paired with re-injection will allow the construction of trace gas analyzers that match or exceed the sensitivity of far more complicated and expensive cavity enhanced methods.

ACKNOWLEDGMENTS

This work was supported under Small Business Innovative Research grants from the U.S. Department of Defense (Grant No. W911SR-09-C-0060) and the National Institutes of Health (Grant No. 1R43ES021129A).

[1]G. Hancock and A. J. Orr-Ewing, in *Cavity Ring-Down Spectrosc: Techniques and Applications*, edited by G. Berden and R. Engeln (Blackwell Publishing Ltd., Washington, D.C., 2009), pp. 181–211.
[2]D. E. Vogler and M. W. Sigrist, Appl. Phys. B **85**, 349 (2006).
[3]L. Pauling, A. B. Robinson, R. Teranishi, and P. Cary, Proc. Natl. Acad. Sci. U.S.A. **68**, 2374 (1971).
[4]W. Cao and Y. Duan, Crit. Rev. Anal. Chem. **37**, 3 (2007).
[5]A. O'Keefe and D. G. Deacon, Rev. Sci. Instrum. **59**, 2544 (1988).
[6]A. O'Keefe, Chem. Phys. Lett. **293**, 331 (1998).
[7]A. O'Keefe, J. J. Scherer, and J. B. Paul, Chem. Phys. Lett. **307**, 343 (1999).
[8]D. S. Baer, J. B. Paul, M. Gupta, and A. O'Keefe, Proc. SPIE **4817**, 167 (2002).
[9]A. Foltynowicz, F. M. Schmidt, W. Ma, and O. Axner, Appl. Phys. B **92**, 313 (2008).
[10]R. Engeln, G. von Helden, G. Berden, G. Meijer, G. Von Helden, G. Berden, and G. Meijer, Chem. Phys. Lett. **262**, 105 (1996).
[11]B. A. Paldus and A. A. Kachanov, Can. J. Phys. **83**, 975 (2005).
[12]J. J. Scherer, J. B. Paul, A. O'Keefe, and R. J. Saykally, Chem. Rev. **97**, 25 (1997).
[13]F. K. Tittel, D. Richter, and A. Fried, in *Topics in Applied Physics*, edited by I. T. Sorokina and K. L. Vodopyanov (Springer-Verlag, Berlin, Heidelberg, 2003), pp. 445–516.
[14]K. E. Whittaker, L. Ciaffoni, G. Hancock, R. Peverall, and G. A. D. Ritchie, Appl. Phys. B **109**, 333 (2012).
[15]J. Peltola, M. Vainio, V. Ulvila, M. Siltanen, M. Metsälä, and L. Halonen, Appl. Phys. B **107**, 839 (2012).
[16]A. Kosterev, G. Wysocki, Y. Bakhirkin, S. So, R. Lewicki, M. Fraser, F. Tittel, and R. F. Curl, Appl. Phys. B **90**, 165 (2008).
[17]M. L. Silva, D. M. Sonnenfroh, D. I. Rosen, M. G. Allen, and A. O'Keefe, Appl. Phys. B **81**, 705 (2005).
[18]R. Provencal, M. Gupta, T. G. Owano, D. S. Baer, K. N. Ricci, A. O'Keefe, and J. R. Podolske, Appl. Opt. **44**, 6712 (2005).
[19]L. Ciaffoni, G. Hancock, J. J. Harrison, J.-P. H. van Helden, C. E. Langley, R. Peverall, G. A. D. Ritchie, S. Wood, and J. H. Van Helden, Anal. Chem. **85**, 846 (2013).
[20]P. Gorrotxategi-Carbajo, E. Fasci, I. Ventrillard, M. Carras, G. Maisons, and D. Romanini, Appl. Phys. B **110**, 309 (2013).
[21]G. N. Rao and A. Karpf, Appl. Opt. **50**, A100 (2011).
[22]Z. Qu, C. Gao, Y. Han, X. Du, and B. Li, Chin. Opt. Lett. **10**, 050102 (2012).
[23]J. A. Decker and H. W. Rogers, in *Ecological Risks Associated with the Destruction of Chemical Weapons*, edited by V. M. Kolodkin and W. Ruck (Springer, Netherlands, 2006), pp. 279–287.
[24]M. B. Pushkarsky, M. E. Webber, T. Macdonald, and C. K. N. Patel, Appl. Phys. Lett. **88**, 044103 (2006).
[25]M. E. Webber, M. Pushkarsky, and C. K. N. Patel, J. Appl. Phys. **97**, 113101 (2005).
[26]J. B. Paul, L. Lapson, and J. G. Anderson, Appl. Opt. **40**, 4904 (2001).
[27]J. B. Leen, X.-Y. Yu, M. Gupta, D. S. Baer, J. M. Hubbe, C. D. Kluzek, J. M. Tomlinson, and M. R. Hubbell, Environ. Sci. Technol. **47**, 10446 (2013).
[28]Y. A. Bakhirkin, A. A. Kosterev, C. Roller, R. F. Curl, and F. K. Tittel, Appl. Opt. **43**(11), 2257 (2004).
[29]C. Dyroff, Opt. Lett. **36**, 1110 (2011).
[30]J. Richter, C. R. Poznich, and D. W. Thomas, Proc. SPIE **1326**, 106–119 (1990).
[31]A. O'Keefe, M. Gupta, T. G. Owano, and D. S. Baer, US patent number 7,468,797 B1 (23 December 2008).
[32]G. P. Eppeldauer and R. J. Martin, J. Res. Natl. Inst. Stand. Technol. **106**, 577 (2001).
[33]P. Zalicki and R. N. Zare, J. Chem. Phys. **102**, 2708 (1995).
[34]K. K. Lehmann and H. Huang, in *Frontiers of Molecular Spectroscopy*, edited by J. Laane (Elsevier, Amsterdam, 2009), pp. 623–658.
[35]D. R. Herriott and H. J. Schulte, Appl. Opt. **4**, 883 (1965).
[36]A. E. Siegman, *Lasers* (University Science Books, Mill Valley, CA, 1986).
[37]J. B. McManus, P. L. Kebabian, and M. S. Zahniser, Appl. Opt. **34**, 3336 (1995).
[38]J. A. Silver, Appl. Opt. **44**, 6545 (2005).
[39]M. Zhao, E. H. Wahl, T. G. Owano, C. C. Largent, R. N. Zare, and C. H. Kruger, Chem. Phys. Lett. **318**, 555 (2000).
[40]S. W. Sharpe, T. J. Johnson, R. L. Sams, P. M. Chu, G. C. Rhoderick, and P. A. Johnson, Appl. Spectrosc. **58**, 1452 (2004).